Vortices in Bose-Einstein condensates: Finite-size effects and the thermodynamic limit

J. C. Cremon,[1] G. M. Kavoulakis,[2] B. R. Mottelson,[3] and S. M. Reimann[1]
[1]*Mathematical Physics, Lund Institute of Technology, P.O. Box 118, SE-22100 Lund, Sweden*
[2]*Technological Education Institute of Crete, P.O. Box 1939, GR-71004, Heraklion, Greece*
[3]*The Niels Bohr International Academy, Blegdamsvej 17, DK-2100 Copenhagen Ø, Denmark*
(Received 30 August 2012; published 22 May 2013)

For a weakly interacting Bose gas rotating in a harmonic trap we relate the yrast states of small systems (that can be treated exactly) to the thermodynamic limit (derived within the mean-field approximation). For a few dozens of atoms, the yrast line shows distinct quasiperiodic oscillations with increasing angular momentum that originate from the internal structure of the exact many-body states. These finite-size effects disappear in the thermodynamic limit, where the Gross-Pitaevskii approximation provides the exact energy to leading order in the number of particles N. However, the exact yrast states reveal significant structure not captured by the mean-field approximation: Even in the limit of large N, the corresponding mean-field solution accounts for only a fraction of the total weight of the exact quantum state.

DOI: 10.1103/PhysRevA.87.053615 PACS number(s): 67.85.De, 05.30.Jp

I. INTRODUCTION

Contrary to many other systems with superfluid properties like, e.g., liquid helium or atomic nuclei, ultracold atomic quantum gases are—at least under typical conditions—very dilute. Still, they may exhibit superfluid properties [1,2] because of their ultralow temperatures. Initial experiments with trapped Bose-Einstein condensates [3–7] have been performed mainly in large systems confining thousands to millions of atoms. It was only more recently that experiments reached the limit of smaller atom numbers $N \sim O(1)$ [8]. In small systems, however, the thermodynamic limit often applied to the case of homogeneous superfluids is not appropriate. Even in the regime of weak interactions, deviations from this limit are expected due to finite-size effects and the influence of the trapping potential.

The rotational properties of Bose-Einstein condensates in a harmonic trap have been studied extensively in the past, see the reviews [9–13]. Previous theoretical studies applied the Gross-Pitaevskii method (for example, [14–18]), or have gone beyond the mean-field approximation (for example, [19–48]). Most of these studies made use of the numerical "exact" diagonalization of the many-body Hamiltonian. Reference [47] and the more recent study in [48] examined the effect of correlations on the rotational properties considering Bogoliubov fluctuations on the mean-field state. Reference [49] went beyond the Bogoliubov description and considered interactions between the quasi-particle excitations.

As discussed below, the exact quantum states of a few dozens of weakly interacting atoms in a rotating harmonic trap reveal significant structure not captured by the Gross-Pitaevskii approximation. It is well known from earlier studies of mean-field theory in the thermodynamic limit that with increasing rotational frequency, a dilute Bose gas in a harmonic trap goes through a systematic series of phase transitions associated with the formation of vortices [14–18]. In the limit of small N, however, finite-size effects become important: Quasiperiodic oscillations occur along the "yrast line" connecting the lowest-energy states as a function of angular momentum ([28,32–35,41,45], see also the discussion in the review articles [11,13]). These oscillations lead to discontinuous steps in the ground state angular momentum L as a function of the trap rotation frequency Ω. They originate from the structure of the exact many-body wave function, generalizing the well-known pattern first described by Butts and Rokshar in the mean-field thermodynamic limit [14]. The Gross-Pitaevskii approximation is known to provide the exact energy to leading order in N [25,50,51]. However, we find that only a fraction of the total weight of the exact quantum state accounts for the corresponding mean-field solution even in the limit of rather large numbers of atoms.

II. MODEL

We consider N bosons of mass M, confined in a harmonic oscillator potential that is isotropic in two dimensions (x,y), with z taken to be the axis of rotation of the cloud. We assume that the system is quasi-two-dimensional, with the motion along the z axis being frozen (i.e., oscillator frequencies $\omega = \omega_x = \omega_y \ll \omega_z$ and $\hbar\omega_z$ larger than the interaction energy). For sufficiently weak interactions one may restrict the set of single-particle states of the harmonic potential to those with zero radial nodes, which is the so-called lowest-Landau-level approximation [9]. Then, the quantum number $m \geqslant 0$ specifying the z component of single-particle angular momentum is the only quantum number defining the orbitals $\psi_{0,m} \propto r^m e^{im\phi} e^{-r^2/2\ell^2}$ (with $\ell = \sqrt{\hbar/M\omega}$). The set $\mathcal{F}$ of Fock states $\{|\Phi_j\rangle\}_{j=1}^{F} = \{|0^{N_0}, 1^{N_1}, \ldots, m^{N_m}\rangle\}_{j=1}^{F}$ (where N_m denotes the number of particles in a single-particle state with angular momentum m) labeled by the index j spans the basis of the many-body state. These Fock states are chosen as eigenstates of the particle-number operator and of the angular-momentum operator, with $\sum_m N_m = N$ as well as $\sum_m m N_m = L$ (units of $\hbar$). In the absence of interactions there is a large degeneracy which comes from the different ways that one may distribute L units of angular momentum to N particles in a harmonic potential [20]. Clearly this degeneracy increases with increasing L and N. In the spirit of degenerate perturbation theory, the Hamiltonian $\hat{H}_{\rm rot}$ is diagonalized in the subspace of these degenerate states. For effective contact interactions between the bosonic

atoms [52], in the rotating frame of reference, $\hat{H}_{\rm rot}$ is given by

$$\hat{H}_{\rm rot} = \hbar\omega N + \hbar(\omega - \Omega)L + \frac{g}{2}\sum_{k\neq l}\delta(\mathbf{r}_k - \mathbf{r}_l), \qquad (1)$$

i.e., only the part coming from the two-body interactions needs to be diagonalized. Here Ω is the trap rotation frequency, and $g = U_0\int|\phi_0(z)|^4\,dz = U_0/(\sqrt{2\pi}\ell_z)$ is the interaction strength, with $\phi_0(z) = e^{-z^2/2\ell_z^2}/(\pi\ell_z^2)^{1/4}$ being the ground state of the potential along the z axis, and ℓ_z is the oscillator length in the z direction. Also, $U_0 = 4\pi\hbar^2 a/M$ is the matrix element for zero-energy elastic two-body collisions between the atoms, with a being the corresponding scattering length. We can thus define the dimensionless parameter $\lambda = NMg/\hbar^2 = \sqrt{8\pi}Na/l_z$ to measure the coupling strength. The eigenstates of $\hat{H}_{\rm rot}$ are expressed as $|L,N\rangle = \sum_{j=1}^{F} C_j \mid \Phi_j\rangle$.

III. RESULTS

It is instructive to start with the case $L/N = 1$, where there is a single vortex state at the center of the cloud, the so-called "unit vortex." Within the mean-field approximation [14,15], all the atoms reside in one single-particle state with $m = 1$. However, the exact many-body wave function (which in this case is known analytically, see [19,21,23]) has a different structure. Although the dominant Fock state corresponds to the mean-field state with macroscopic occupancy of the $m = 1$ orbital, in addition there are orbitals with $m = 0$ and $m = 2$. The yrast state of the unit vortex can be written as [15,19] $|L = N,N\rangle = \sum_k(-1)^k C_k|0^k,1^{N-2k},2^k\rangle$, where $C_k = 1/(\sqrt{2}^{k+1})$ to leading order in N. The component corresponding to the mean-field approximation is the single term with $k = 0$, with $|C_0|^2 = 1/2$. All other Fock states, with their sum trivially adding up to completeness, $\sum_{k\neq 0}|C_k|^2 = 1/2$, have significantly smaller amplitudes. In other words, half of the weight of the total wave function is not captured by the single dominant Fock state carrying a macroscopic occupancy that corresponds to the mean-field solution. (For a discussion of the unit vortex see also Refs. [21,46,47].) Evaluating the mean occupancy of the three single-particle states from the exact state, one finds [19] that to leading order in N, the occupancy of the $m = 1$ state is $\langle N_1\rangle = N - 2$, while for $m = 0$ and $m = 2$ we have $\langle N_0\rangle = \langle N_2\rangle = 1$. (The mean occupancy of all other single-particle states is of lower order in N, which justifies to neglect them.) Thus, there is only one single-particle orbital that is macroscopically occupied for large N. The depletion of the condensate, defined as $(\langle N_0\rangle + \langle N_2\rangle)/N$, equals $2/N$. In the mean-field approximation the energy (in the laboratory frame of reference) at $L/N = 1$ is $\mathcal{E}_{\rm MF} = N\hbar\omega + gN(N-1)/2$ (see [15]), while the exact energy is $\mathcal{E}_{\rm ex} = N\hbar\omega + gN(N-2)/2$ (see [19,21]). The comparison shows that the mean-field energy is correct to leading order in N, while the contribution of the single-particle states $m = 0$ and $m = 2$ that are absent in the mean-field solution give corrections to the energy that are of lower order in N [25].

Beyond the unit vortex, for $L/N > 1$ the yrast states are not analytically known, and one needs to turn to numerical methods instead. The upper panel of Fig. 1 shows the yrast energies (in the rotating frame) obtained by the Gross-Pitaevskii method

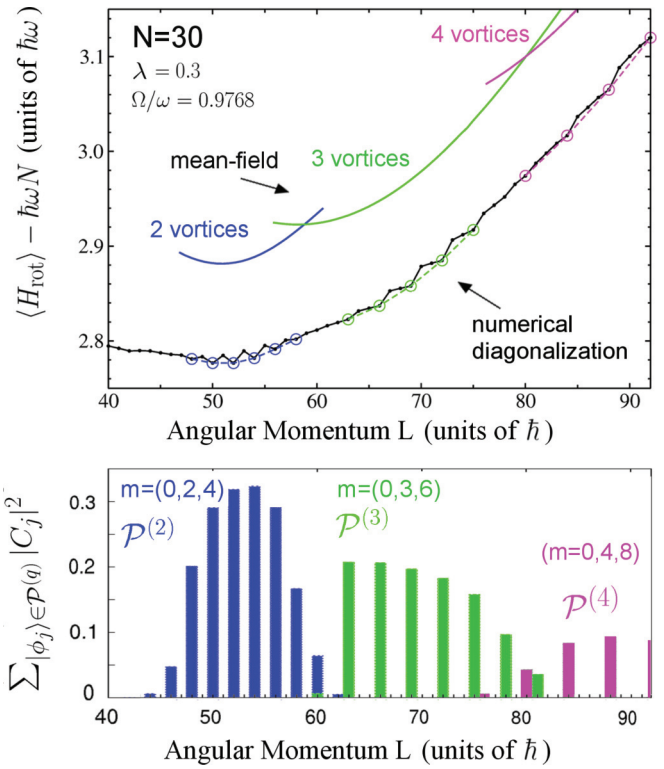

FIG. 1. (Color online) Comparison of mean-field and "exact" yrast states of $N = 30$. *Upper panel:* Energy (in the rotating frame) as a function of total angular momentum L, at a rotational frequency of $\Omega/\omega = 0.9768$, and a coupling strength $\lambda = 0.3$. The black line shows the result of the numerical diagonalization. Cusps in the yrast line occur with a quasiperiodicity of $q = 2$, 3, and 4 in L, as marked by the *blue*, *green*, and *magenta* circles. The three higher-energy parabolas show the result of the corresponding mean-field variational calculation. *Lower panel:* Sum $\sum_{|\Phi_j\rangle\in\mathcal{P}(q)}|C_j|^2$ of amplitudes of Fock states $|\Phi_j\rangle$ built exclusively out of the orbitals that are macroscopically occupied within the mean-field approximation (see text), with $(m = 0,2,4)$, $(m = 0,3,6)$, and $(m = 0,4,8)$ for the cases of twofold (*blue*, $q = 2$), threefold (*green*, $q = 3$), and fourfold (*magenta*, $q = 4$) symmetry, respectively.

(upper, parabolic lines), in comparison to the energies obtained by exact diagonalization (lower black line), calculated for $N = 30$, for the interaction strength $\lambda = 0.3$, and $\Omega/\omega = 0.9768$.[1]

For $1.7 \lesssim L/N \lesssim 2.03$, the yrast state consists of single-particle orbitals with even values of m, and thus has twofold symmetry. The occupancy of the orbitals with odd m is of lower order in N, and thus negligible in the thermodynamic limit assumed within the mean-field approximation [15]. For the simple form $\Psi = c_0\psi_{0,0} + c_2\psi_{0,2} + c_4\psi_{0,4}$, the mean-field energy is straightforwardly obtained variationally under the constraints of fixed particle number and of fixed expectation value of angular momentum. For twofold symmetry, the corresponding energy is shown as the upper blue line in Fig. 1. Similarly, we may evaluate the energies for the order parameter with threefold symmetry (green line), consisting

[1]Here, up to $m \leqslant 14$ single-particle orbitals were included in the basis states. For diagonalization we used the ARPACK library.

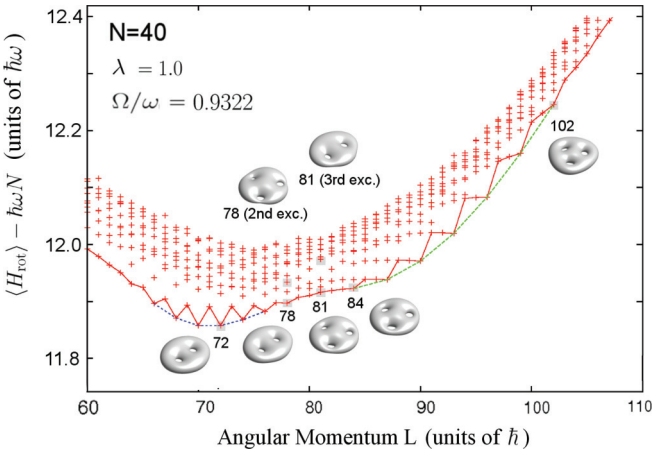

FIG. 2. (Color online) The energy of the yrast state and of the low-lying excited states in the rotating frame for $N = 40$, $\Omega/\omega = 0.9322$, and $\lambda = 1.0$. Insets: Isosurfaces (placed at half-maximum value) of the pair-correlated densities; reference point in the (x,y) plane at (1,0). [Units of the oscillator length $(\hbar/M\omega)^{1/2}$] (see text).

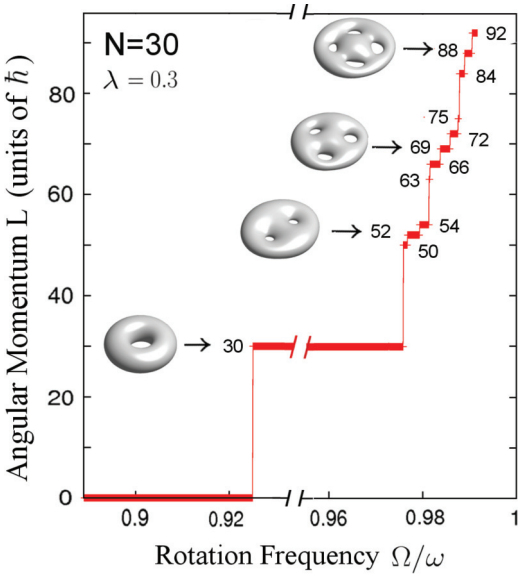

FIG. 3. (Color online) Angular momentum $L = L(\Omega/\omega)$ resulting from minimizing $E_0^{\rm rot}$ for $N = 30$ and $\sqrt{8\pi}Na/l_z = 0.3$, showing additional steps in L that originate from the quasiperiodicity of the yrast line. The insets show isosurfaces of the pair-correlated densities (as in Fig. 2).

exclusively of single-particle orbitals with angular momenta m that are multiples of three, $\Psi = c_0\psi_{0,0} + c_3\psi_{0,3} + c_6\psi_{0,6}$, and fourfold symmetry (gray line) with m being multiples of four, $\Psi = c_0\psi_{0,0} + c_4\psi_{0,4} + c_8\psi_{0,8}$. The local energy minima associated with a given symmetry in the order parameter compete with each other, giving rise to the discontinuous phase transitions between states of different symmetry as Ω increases.

For finite N, the *exact* energy (shown by the black line in Fig. 1) overall lies below the mean-field value, as expected. The yrast line shows oscillations with a quasiperiodicity increasing from $q = 2$ to 3, and then 4 units of angular momentum (for the range of L considered here). We find that the minima (downward cusps, marked by circles) occurring with quasiperiodicity q lie on parabolic energy branches that are associated with the symmetry of the yrast states, similar to the Gross-Pitaevskii mean-field result. The crossings between the different branches mark the transitions between the different symmetries.

Figure 2 shows the yrast line and low-lying excitations in the rotating frame for $N = 40$ particles, for $\lambda = 1.0$, and $\Omega/\omega = 0.9322$ (here for a basis with $m \leqslant 12$), where similar oscillations occur (here only shown up to $q = 3$ due to the rapid increase in matrix dimension for larger N). The insets to Fig. 2 show the isodensity surfaces of the pair-correlated densities [defined as $\langle\Psi|\hat{\Psi}^\dagger(\mathbf{r})\hat{\Psi}^\dagger(\mathbf{r}')\hat{\Psi}(\mathbf{r}')\hat{\Psi}(\mathbf{r})|\Psi\rangle$]. Around the transition between two and three vortices (see insets) it is apparent that there is a crossing of states.

Let us now further analyze the quasiperiodicity of the yrast line for the example of the two-vortex state. If N is even and L is a multiple of 2 (but not of 4), then the Fock states $|k\rangle$ with the largest amplitudes giving rise to the downward cusps have the form

$$|0^{k+N/2-(L+2)/4}, 2^{N+1-2k}, 4^{k-N/2+(L-2)/4}\rangle. \tag{2}$$

If L is a multiple of 4, then the corresponding states are

$$|0^{k+N/2-L/4}, 2^{N-2k}, 4^{k-N/2+L/4}\rangle. \tag{3}$$

The integer k takes all the possible values for which the occupancies are non-negative.

The quasiperiodic oscillations give rise to the additional distinct steps (as in this case, of two units in L in the region of the two-vortex state) in the graph $L(\Omega)$ that is obtained by minimizing the energy at a given value of Ω in the rotating frame, see Fig. 3. A similar situation occurs for the vortex states with three- and fourfold symmetry, giving rise to the corresponding quasiperiodicity in the yrast energy, as well as the steps in $L(\Omega)$. These additional steps disappear in the thermodynamic limit and the curve becomes a piecewise continuous function of Ω, as described by Butts and Rokshar [14]. Along the steps, the pair-correlated densities (shown as isosurfaces in the insets to Fig. 3) follow a pattern similar to the mean-field results [14].

In the mean-field solution, for a given symmetry only a certain subset of single-particle states with angular momentum m contribute to the order parameter [15]. The whole Fock space $\mathcal{F}$ may thus be viewed as composed of a subspace $\mathcal{P}^{(q)}$ that is exclusively built on the Fock states constructed with single-particle orbitals that appear in the mean-field solution [as for two-, three-, or fourfold symmetry, $q = 2$, 3, or 4, these are only the orbitals with $m = (0,2,4)$, $m = (0,3,6)$, and $m = (0,4,8)$, respectively], and the rest of all the Fock states building a space that we call $\mathcal{Q}^{(q)}$. Obviously, $\mathcal{F} = \mathcal{P}^{(q)} \cup \mathcal{Q}^{(q)}$. [For the two-vortex case, the Fock states in $\mathcal{P}^{(2)}$ were given in Eqs. (2) and (3) above.] For a diagonalization within $\mathcal{P}^{(q)}$ only, one obtains the exact leading-order term in the energy [25]. The contribution of all other Fock states that are elements of $\mathcal{Q}^{(q)}$ lowers the energy to subleading order in N. [As an example, in the truncated space $m = (0,2,4)$, diagrams which contribute to subleading order in N are shown in Fig. 4(a) where the contribution of the states with $m = 1$ and $m = 3$ may be considered perturbatively.] The sum of amplitudes of all

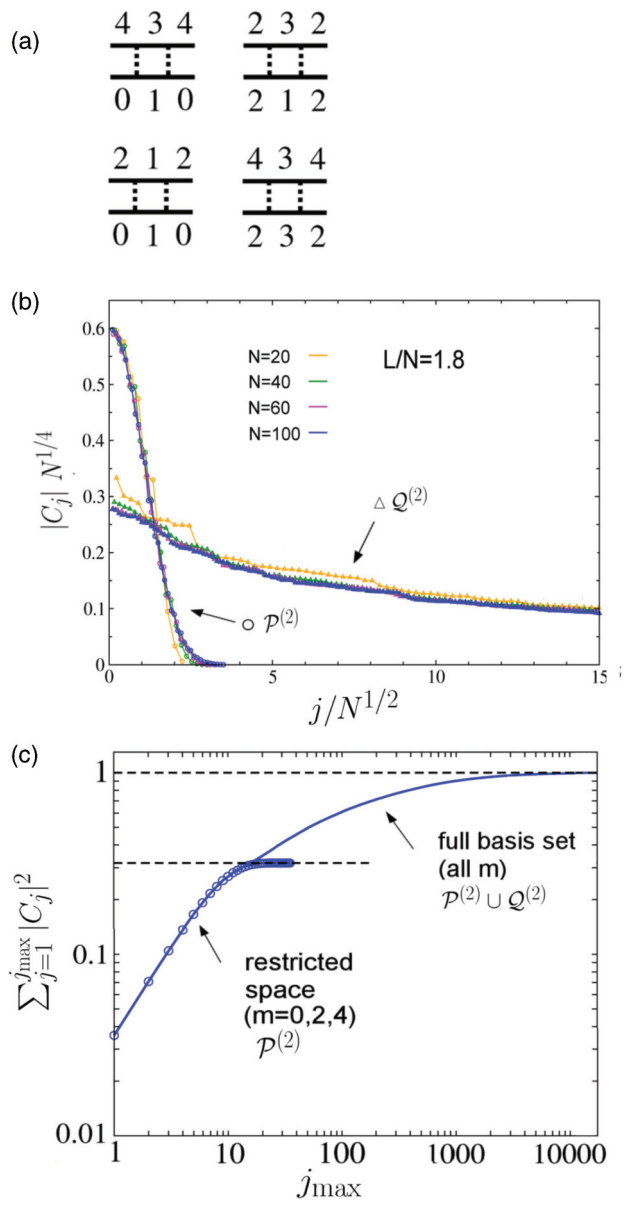

FIG. 4. (Color online) Comparison between the restricted and the complementary Fock space for the two-vortex state at $L/N = 1.8$. (a) Diagrams showing the contributions to subleading order in N, here for $m \leqslant 4$. (b) Amplitudes in the subspaces $\mathcal{P}^{(2)}$ and $\mathcal{Q}^{(2)}$, ordered after their absolute size. (c) Saturation of the sum of amplitudes $\sum_{j=1}^{j_{max}} |C_j|^2$ (here for $N = 100$) in $\mathcal{P}^{(2)}$ to about 30% of the full weight.

Fock states that are in $\mathcal{P}^{(q)}$ is plotted in the lower panel of Fig. 1 for those states that are downward cusps in the yrast line for $q = 2$, 3, and 4. The amplitude sums practically vanish around the transitions between different values of q where the exact yrast states become very mixed, i.e., there is a superposition of very many Fock states with comparable and small amplitudes.

Remarkably, around angular momenta where vortex states with a given symmetry occur as ground states, the subspace $\mathcal{P}^{(q)}$ adds up to only a fraction of the total weight of the exact quantum state. For the unit vortex with $q = 1$, as discussed above, there is a single term $|0,1^N,0,0,\ldots\rangle$ that has 50% of the total amplitude. For $q = 2$, only about 30% of the total amplitude is within $\mathcal{P}^{(2)}$, while the contribution of the majority of Fock states that belong to $\mathcal{Q}^{(2)}$ amounts to the remaining 70%. For $q = 3$, the weight of the restricted subspace $\mathcal{P}^{(3)}$ decreases to about 20%, and for $q = 4$ we obtain only about 10% in $\mathcal{P}^{(4)}$.

The ratio between the weights of $\mathcal{P}^{(q)}$ and $\mathcal{Q}^{(q)}$ does not appear to be a finite-N effect, but systematically persists for larger system sizes.[2] This becomes particularly clear when studying the Fock state amplitudes in the different subspaces. For the two-vortex state at $L/N = 1.8$ for $N = 20$, 40, 60, and 100 particles,[3] Fig. 4(b) shows the absolute values of the amplitudes (ordered after their absolute size) that are found to scale with the particle number as $N^{1/4}$, as a function of the Fock space index j, that scales as $1/N^{1/2}$, for the subspaces $\mathcal{P}^{(2)}$ (which is relatively small in dimension) and $\mathcal{Q}^{(2)}$ (which is huge, containing very many states with small amplitudes). Figure 4(c) shows the corresponding sums of the squared amplitudes $\sum_{j=1}^{j_{max}} |C_j|^2$ (here only for $N = 100$) in $\mathcal{P}^{(2)}$ and $\mathcal{F} = \mathcal{P}^{(2)} \cup \mathcal{Q}^{(2)}$. The sum in $\mathcal{F}$ quickly saturates to unity, while in the restricted space $\mathcal{P}^{(2)}$ it saturates to only about 30% of the total weight of the quantum state. We see that for particle numbers $N \geqslant 40$, the scaling in N becomes nearly perfect, indicating that the distribution of states between $\mathcal{P}$ and $\mathcal{Q}$ would not change when going to even larger particle numbers.

IV. CONCLUSION

To conclude, using the method of numerical diagonalization for a few dozens of atoms rotating in a harmonic trap, we found that quasiperiodic oscillations along the yrast line originate from the finiteness of the system, and disappear in the mean-field limit of large N. Furthermore, comparing the yrast state in the restricted subspace corresponding to the mean-field solution, with the exact yrast state in the full space, we found that it accounts for only a fraction of the total weight. There is additional structure in the exact state that persists when the system approaches the limit of large N, even though the mean-field approximation provides the yrast energy exactly in this limit.

ACKNOWLEDGMENTS

We thank A. D. Jackson, M. Manninen, C. J. Pethick, C. Verdozzi, A. Wacker, and S. Åberg for discussions and useful input. This work was financially supported by the Swedish Research Council and the Nanometer Structure Consortium at Lund University, as well as the POLATOM ESF research networking programme.

[2]We varied the particle number from $N = 20$ which is sufficiently small to be treated with no truncation, up to about $N = 100$, where we were limited to only $m \leqslant 7$ orbitals. In this range of particle numbers, we found that the sum of the amplitudes in $\mathcal{P}^{(2)}$ shows only a very small decrease of at most 1%, a value close to the limit of accuracy caused by the unavoidable truncation of the single-particle basis states in the case of large N and L.

[3]For $N \leqslant 40$ we used a truncation of $m \leqslant 14$, for $N \leqslant 70$, $m \leqslant 9$, and for $N = 100$, $m \leqslant 7$ single-particle orbitals.

[1] A. J. Leggett, Rev. Mod. Phys. **71**, 318 (1999).
[2] A. J. Leggett, Rev. Mod. Phys. **73**, 307 (2001).
[3] K. B. Davis, M. O. Mewes, M. A. Joffe, M. R. Andrews, and W. Ketterle, Phys. Rev. Lett. **74**, 5202 (1995).
[4] K. B. Davis, M.-O. Mewes, M. R. Andrews, N. J. van Druten, D. S. Durfee, D. M. Kurn, and W. Ketterle, Phys. Rev. Lett. **75**, 3969 (1995).
[5] M. Andersson, J. Ensher, M. Matthews, C. Wieman, and E. Cornell, Science **269**, 198 (1995).
[6] E. Cornell and C. Wieman, Rev. Mod. Phys. **74**, 875 (2002).
[7] W. Ketterle, Rev. Mod. Phys. **74**, 1131 (2002).
[8] F. Serwane, G. Zurn, T. Lompe, T. B. Ottenstein, A. N. Wenz, and S. Jochim, Science **332**, 336 (2011).
[9] A. Fetter, Rev. Mod. Phys. **81**, 647 (2009).
[10] I. Bloch, J. Dalibard, and W. Zwerger, Rev. Mod. Phys. **80**, 885 (2008).
[11] N. R. Cooper, Adv. Phys. **57**, 539 (2008).
[12] S. Viefers, J. Phys.: Condens. Matter **20**, 123202 (2008).
[13] H. Saarikoski, S. Reimann, A. Harju, and M. Manninen, Rev. Mod. Phys. **82**, 2785 (2010).
[14] D. Butts and D. Rokshar, Nature (London) **397**, 327 (1999).
[15] G. M. Kavoulakis, B. Mottelson, and C. J. Pethick, Phys. Rev. A **62**, 063605 (2000).
[16] M. Linn and A. L. Fetter, Phys. Rev. A **60**, 4910 (1999).
[17] M. Linn, M. Niemeyer, and A. L. Fetter, Phys. Rev. A **64**, 023602 (2001).
[18] J. J. García-Ripoll and V. M. Pérez-García, Phys. Rev. A **63**, 041603(R) (2001).
[19] N. K. Wilkin, J. M. F. Gunn, and R. A. Smith, Phys. Rev. Lett. **80**, 2265 (1998).
[20] B. Mottelson, Phys. Rev. Lett. **83**, 2695 (1999).
[21] G. F. Bertsch and T. Papenbrock, Phys. Rev. Lett. **83**, 5412 (1999).
[22] A. D. Jackson and G. M. Kavoulakis, Phys. Rev. Lett. **85**, 2854 (2000).
[23] R. A. Smith and N. K. Wilkin, Phys. Rev. A **62**, 061602 (2000).
[24] N. R. Cooper, N. K. Wilkin, and J. M. F. Gunn, Phys. Rev. Lett. **87**, 120405 (2001).
[25] A. D. Jackson, G. M. Kavoulakis, B. Mottelson, and S. M. Reimann, Phys. Rev. Lett. **86**, 945 (2001).
[26] M. Manninen, S. Viefers, M. Koskinen, and S. M. Reimann, Phys. Rev. B **64**, 245322 (2001).
[27] M. Ueda and T. Nakajima, Phys. Rev. A **64**, 063609 (2001).
[28] X.-J. Liu, H. Hu, L. Chang, W. Zhang, S.-Q. Li, and Y.-Z. Wang, Phys. Rev. Lett. **87**, 030404 (2001).
[29] T. Nakajima and M. Ueda, Phys. Rev. A **63**, 043610 (2001).
[30] T. Nakajima and M. Ueda, Phys. Rev. Lett. **91**, 140401 (2003).
[31] I. Romanovsky, C. Yannouleas, and U. Landman, Phys. Rev. Lett. **93**, 230405 (2004).
[32] M. Manninen, S. M. Reimann, M. Koskinen, Y. Yu, and M. Toreblad, Phys. Rev. Lett. **94**, 106405 (2005).
[33] S. M. Reimann, M. Koskinen, Y. Yu, and M. Manninen, Phys. Rev. A **74**, 043603 (2006).
[34] S. M. Reimann, M. Koskinen, Y. Yu, and M. Manninen, New J. Phys. **8**, 59 (2006).
[35] N. Barberán, M. Lewenstein, K. Osterloh, and D. Dagnino, Phys. Rev. A **73**, 063623 (2006).
[36] I. Romanovsky, C. Yannouleas, L. O. Baksmaty, and U. Landman, Phys. Rev. Lett. **97**, 090401 (2006).
[37] M. Ueda and T. Nakajima, Phys. Rev. A **73**, 043603 (2006).
[38] C. Yannouleas and U. Landman, Rep. Prog. Phys. **70**, 2067 (2007).
[39] D. Dagnino, N. Barberán, K. Osterloh, A. Riera, and M. Lewenstein, Phys. Rev. A **76**, 013625 (2007).
[40] N. Hamamoto, M. Oi, and N. Onishi, Phys. Rev. A **75**, 063614 (2007).
[41] I. Romanovsky, C. Yannouleas, and U. Landman, Phys. Rev. A **78**, 011606 (2008).
[42] M. I. Parke, N. K. Wilkin, J. M. F. Gunn, and A. Bourne, Phys. Rev. Lett. **101**, 110401 (2008).
[43] D. Dagnino, N. Barberán, M. Lewenstein, and J. Dalibard, Nat. Phys. **5**, 431 (2009).
[44] D. Dagnino, N. Barberán, and M. Lewenstein, Phys. Rev. A **80**, 053611 (2009).
[45] Z. Liu, H. Guo, S. Chen, and H. Fan, Phys. Rev. A **80**, 063606 (2009).
[46] A. Nunnenkamp, A. Rey, and K. Burnett, Proc. R. Soc. A Math. Phys. Eng. **466**, 1247 (2010).
[47] S. Baharian and G. Baym, Phys. Rev. A **82**, 063606 (2010).
[48] S. Baharian and G. Baym, Phys. Rev. A **87**, 033619 (2013).
[49] M. P. Kwasigroch and N. R. Cooper, Phys. Rev. A **86**, 063618 (2012).
[50] E. H. Lieb, R. Seiringer, and J. Yngvason, Phys. Rev. A **61**, 043602 (2000).
[51] E. H. Lieb, R. Seiringer, and J. Yngvason, Phys. Rev. A **79**, 063626 (2009).
[52] M. Lewin and R. Seiringer, J. Stat. Phys. **137**, 1040 (2009).